PHYSICAL REVIEW A VOLUME 20, NUMBER 1 JULY 1979

Approach to electron capture into arbitrary principal shells of energetic projectiles

Jörg Eichler* and F. T. Chan†
Bereich Kern-und Strahlenphysik, Hahn-Meitner-Institut für Kernforschung Berlin GmbH, D-1000 Berlin-39, Federal Republic of Germany
(Received 28 February 1979)

An approach for treating electron capture into arbitrary principal shells or into continuum states of energetic projectiles is developed. The approach is based on the momentum-density matrix of the captured electron summed over all substates l, m or integrated over all emission angles, respectively. In conjunction with the kinematics of energetic capture reactions it leads to drastic simplifications in capture theories. Within the eikonal approximation, the present approach yields an exact result for the cross section describing capture of hydrogenic 1s electrons into hydrogenic bound or continuum states of the projectile. The final result is a simple analytical expression factorizing into the Oppenheimer-Brinkman-Kramers cross section times a scaling factor between 0.1 and 0.4. The theoretical scaling factor for the total cross section turns out to be a function of v/v_K (the ratio of projectile velocity to target K-shell velocity) which is approximately independent of the target and projectile charges. For hydrogen and helium targets surprisingly good agreement is obtained with a large body of experimental data.

I. INTRODUCTION

The capture of 1s electrons in collisions of energetic multiply charged ions with light target atoms is of considerable interest both in terms of basic theory and in various practical applications. In particular, electron capture from hydrogen (and deuterium) is relevant for astrophysical plasmas and for magnetically confined fusion plasmas heated by a neutral hydrogen beam.

The theoretical investigations[1-3] have been mostly confined to capture from hydrogen atoms into 1s states of H^+ projectiles. Very few studies have been made of capture into multiply charged heavier ions. This is so because with increasing projectile charge the electrons are captured into increasingly higher principal shells n of the projectile. Such high quantum states present formidable difficulties to a quantum treatment. A striking exception in simplicity is provided by the Oppenheimer-Brinkman-Kramers (OBK) approximation.[1,2,4,5] In this particular case, a sum rule first given by Fock[6] allows one to carry out the subshell summations and to derive a closed-form expression.[4] It is well known[7] that the OBK approximation considerably overestimates the experimental total cross section but otherwise reflects the correct behavior. It therefore has become a common practice[1,7] to scale the OBK cross section down by an empirical factor $\alpha(v)=0.1-0.4$ independent of the projectile charge Z_p. So far it is not fully understood why this scaling procedure works so well.

As an alternative approach to charge capture (and ionization), the classical-trajectory Monte Carlo method has been applied by Olson and Salop[8] and by Olson *et al.*[9] to a large variety of heavy highly charged ions colliding with hydrogen atoms. The method has proven to be surprisingly successful[9] in reproducing the experimental electron-loss data in the energy range 50–5000 keV/amu.

The common source of the successes of the classical calculations and (to a limited extent) of the OBK approximation probably lies in the fact that charge capture at high projectile energies is largely governed by the initial and final *momentum distribution* of the electrons. In fact, the classical momentum distribution of a microcanonical ensemble of electrons[1,2] with energies $E_n = -\frac{1}{2}Z^2/n^2$ is identical to the quantal momentum distribution.[10] This is well known[1,2] for $n=1$, but—owing to the $O(4)$ symmetry of the hydrogen problem[6]—also holds[10] for arbitrary principal shells n after summation over the n^2 substates[6] (see Sec. II). It is just this sum rule on which the OBK approximation for higher n is based.[4] In general, it is to be expected that any theoretical treatment paying sufficient attention to the momentum distribution will meet a certain amount of success in predicting total capture cross sections.

In a previous paper[10] we have exploited this idea. In the present work we extend the treatment and give a more detailed derivation. We also discovered that our previous result is *exact* within the eikonal approximation.

II. THEORETICAL BACKGROUND FOR ELECTRON CAPTURE INTO PRINCIPAL SHELL n

A. Density matrix in momentum space

As early as 1935, Fock published a fundamental paper[6] proving that for the hydrogen atom the solutions of the Schrödinger equation in momentum space are proportional to four-dimensional spherical harmonics. Defining these solutions as the Fourier transforms

$$\tilde{\varphi}_{nlm}(\vec{q}) = (2\pi)^{-3/2} \int d^3r\, \varphi_{nlm}(\vec{r}) \exp(i\vec{q}\cdot\vec{r}) \tag{1}$$

of the normalized hydrogenic wave functions $\varphi_{nlm}(\vec{r})$ and introducing the momentum-density matrix of the nth principal shell as

$$\rho_n(\vec{q},\vec{q}\,') = \sum_{l=0}^{n-1} \sum_{m=-l}^{l} \tilde{\varphi}^*_{nlm}(\vec{q})\tilde{\varphi}_{nlm}(\vec{q}\,'), \tag{2}$$

Fock's result immediately implies the existence of an addition theorem[6] which allows one to rewrite Eq. (2) in the form

$$\rho_n(\vec{q},\vec{q}\,') = \frac{8n^2 q_n^5}{\pi^2(q^2+q_n^2)^2(q'^2+q_n^2)^2}\,\frac{\sin nx}{n\sin x}. \tag{3}$$

Here $q_n = Z/n$ and x denotes a distance on a four-dimensional unit spere which, via the familiar relation

$$\cos x = \cos\theta\,\cos\theta' + \sin\theta\,\sin\theta'\cos\gamma \tag{4}$$

is expressed by the angle γ between the vectors $\vec{q}$ and $\vec{q}\,'$ and by their "polar angles" θ and θ' with respect to the fourth axis (in addition to the three axes in momentum space). The angles are defined by

$$\cos\theta = \frac{q_n^2 - q^2}{q_n^2 + q^2}, \quad \sin\theta = \frac{2qq_n}{q_n^2 + q^2}, \tag{5}$$

and analogous relations for θ'.

Equation (3) has been used by Omidvar[11] in his Born treatment of electron capture into states with asymptotically high n but otherwise has not received much attention, possibly owing to the difficulty to visualize four-dimensional space. However, it may be cast into a form[10] more readily applicable to physical problems by inserting Eqs. (5) and the definition of γ so that

$$\sin\tfrac{1}{2}x = \pm q_n|\vec{q}-\vec{q}\,'|/[(q^2+q_n^2)(q'^2+q_n^2)]^{1/2} \tag{6}$$

directly exhibits its dependence on the "momentum spread" $|\vec{q}-\vec{q}\,'|$. Using Eq. (6) it is easily seen that the function $d_n(x) = \sin nx/(n\sin x)$ reaches the peak value $d_n(0)=1$ for $\vec{q}=\vec{q}\,'$ and a backward peak $d_n(\pi) = (-1)^{n+1}$ at $\vec{q}=-\vec{q}\,'$. The width of the peak is proportional to $1/n$.

An expression similar to Eq. (3) may be obtained[4] for the function

$$g_{nlm}(\vec{q}) = (2\pi)^{-3/2} \int \frac{d^3r}{r}\varphi_{nlm}(\vec{r}) \exp(i\vec{q}\cdot\vec{r}) \tag{7}$$

by inserting φ_{nlm} into the Schrödinger equation. This leads to the sum rule

$$\sum_{lm} g^*_{nlm}(\vec{q})g_{nlm}(\vec{q}\,') = \frac{2q_n^3}{\pi^2(q^2+q_n^2)(q'^2+q_n^2)}\,\frac{\sin nx}{n\sin x}. \tag{8}$$

B. Approximation scheme for electron capture

In principle, any reaction involving the nth principal shell could be treated in momentum space using expression (3) to evaluate the double-momentum integrals $\int d^3q \int d^3q'$ determining the cross section. In general, the momenta $\vec{q}$ and $\vec{q}\,'$ are coupled by the function $d_n(x) = \sin nx/(n\sin x)$ and hence the evaluation is complicated. In the particular case of electron capture by energetic projectiles, however, one has an enormously simplifying feature: The momentum distribution of the captured electron is almost exclusively determined by the prescribed relative velocity $\vec{v}$ of the colliding nuclei.[12] That is, one will only have contributions to the cross section from the domain in double momentum space defined by $\vec{q}\approx\vec{q}\,'$.

It is instructive to estimate the argument x of $d_n(x)$ for a given projectile charge Z and impact parameter b. The transverse momentum transfer is classically given by $q_\perp = 2Z/(vb)$. Taking $q_\parallel \approx v > q_n$, $|\vec{q}-\vec{q}\,'| \approx q_\perp$, and $q^2 \approx q'^2$, we estimate from Eq. (6), $|\sin\frac{1}{2}x| < 2Z^2/(nv^3b) \approx 2Z^3/(n^3v^3)$, where, in the last equality, we have assumed that the typical impact parameter equals the Bohr radius of the orbit into which the electron is captured. If the parameters in this estimate are such that x is much smaller than the width $1/n$ of $d_n(x)$ it is a good approximation to put $d_n(x)=1$. Because of the v^{-3} dependence this may already be fulfilled at moderate collision velocities.

Given the specific kinematic conditions of electron capture it will have no effect on the calculated cross section if density matrix (3) or (8) is arbitrarily altered in the whole $\vec{q},\vec{q}\,'$ space except in the domain $\vec{q}\approx\vec{q}\,'$. We may therefore substitute an effective density matrix

$$\rho_n^{\text{capt}}(\vec{q},\vec{q}\,') = \frac{2^{3/2}nq_n^{5/2}}{\pi(q^2+q_n^2)^2}\,\frac{2^{3/2}nq_n^{5/2}}{\pi(q'^2+q_n^2)^2} \tag{9}$$

and a similar relation corresponding to Eq. (8). Obviously, ρ_n^{capt} factorizes into two $1s$ wave functions in momentum space

$$\varphi_n^{\text{capt}}(Z) = n\varphi_{1s}(Z/n). \tag{10}$$

We may, therefore, formulate an approximation scheme[10] which drastically simplifies the computation of electron capture into arbitrary principal shells: The total cross section for electron capture into the nth principal shell (summed over all l, m substates) of a projectile with charge Z can be calculated as the capture into the $1s$ state of a substitute projectile with charge Z/n by using Eq. (10) in momentum or in coordinate space.

The arguments given above are independent of the specific approach taken to calculate capture cross sections. We discovered, however, that in the eikonal approach described in Sec. III the prescription to take $\vec{q}=\vec{q}'$ or $x=0$ is not an approximation but holds exactly.

III. ELECTRON CAPTURE IN THE EIKONAL APPROXIMATION

Here we want to apply the general ideas outlined in Sec. II to the eikonal (or Glauber) approximation.[13] This approximation requires[13] that the collision time $\tau_{\text{coll}} \approx 2a_K/v$ (where a_K is the Bohr radius of the initially bound electron) be small compared to the typical transition time $\tau_{\text{trans}} \approx 2\pi/\epsilon$ (where ϵ is the transition frequency or energy difference in atomic units between initial and final electronic states). Introducing the target charge number Z_t and $\eta = 1/v$ we therefore require

$$\tau_{\text{coll}}/\tau_{\text{trans}} \approx (1/\pi)(\epsilon/Z_t)\eta \ll 1 . \tag{11}$$

This condition may be fulfilled even at comparatively low velocities if the "resonant" capture with $\epsilon \approx 0$ dominates the cross section. In the following, we first consider capture into bound states and then show that the same methods may be applied to capture into the continuum of the projectile.

A. Cross section for capture into bound states

We now proceed to calculate in some detail the capture of an electron initially bound in the $1s$ shell of a hydrogenic target with charge Z_t into the nth principal shell of a bare projectile ion with charge Z_p.

The eikonal approximation has been first applied by Tsuji and Narumi[14] and by Dewangan[15] to electron capture from hydrogen atoms into $1s$ states of hydrogen ions. We generalize the treatment to arbitrary principal shells n which for high-Z projectiles dominate the total capture cross section. It should be mentioned, at this point, that with increasing n the initial and final bound states become more and more orthogonal and hence the problem of whether or not to include the internuclear interaction in the transition amplitude does not arise. Let $\vec{r}$, $\vec{r}_t = \vec{r} + \alpha\vec{R}$, and $\vec{r}_p = \vec{r} - (1-\alpha)\vec{R}$ denote the position of the electron with respect to the center of mass, the target, and the projectile nucleus, respectively, with $\alpha = M_p/(M_p+M_t)$. The projectile is assumed to follow a straight-line trajectory $\vec{R} = \vec{b} + \vec{z}_R$ with respect to the target nucleus. In order to take advantage of sum rule (8) it is convenient to adopt the eikonal approximation in its *prior* form. The transition amplitude is then given by

$$A_{1s\text{-}nlm}(\vec{b}, v) = -i \int_{-\infty}^{\infty} dt \langle \Psi_t | (-Z_p/r_p) | \Psi_{1s} \rangle . \tag{12}$$

Introducing the energies $\epsilon_t = -\frac{1}{2}Z_t^2$ and $\epsilon_p = -\frac{1}{2}Z_p^2/n^2$, and using the conventional translation factors[1] we can specify the time-dependent wave functions as

$$\Psi_{1s} = \varphi_{1s}(\vec{r}_t) \exp(-i\epsilon_t t) \times \exp(-i\alpha\vec{v}\cdot\vec{r} - \tfrac{1}{2}i\alpha^2 v^2 t) \tag{13}$$

and

$$\Psi_f = \varphi_{nlm}(\vec{r}_p) \exp(-i\epsilon_p t) \times \exp[i(1-\alpha)\vec{v}\cdot\vec{r} - \tfrac{1}{2}i(1-\alpha)^2 v^2 t] \times \exp\left(-i \int_t^{\infty} \frac{Z_t'}{r_t} dt'\right) . \tag{14}$$

The last factor in Ψ_f represents the eikonal phase factor in the *prior* form.[16] For the application to multielectron targets we allow here the effective charge Z_t' in the final state to be different from the charge Z_t in the initial state. Using the integral representation given by Gau and Macek[15b] we can rewrite the phase factor as

$$\exp\left(i \int_t^{\infty} \frac{Z_t'}{r_t} dt'\right) = \exp[i\eta Z_t' \ln(r_t - z_t)] = \frac{1}{\Gamma(-i\eta Z_t')} \int_0^{\infty} \lambda^{-i\eta Z_t' - 1} \times \exp[-\lambda(r_t - z_t)]\, d\lambda . \tag{15}$$

After inserting Eqs. (13) and (14) into Eq. (12) we may express the functions $\varphi_{nlm}(\vec{r}_p)/r_p$ by their Fourier transforms defined in Eq. (7). Furthermore, the exponentials occuring in $\varphi_{1s}(\vec{r}_t) = \pi^{-1/2} Z_t^{3/2} \exp(-Z_t r_t)$ and in representation (15) of the eikonal phase may be combined to give

$$e^{-(\lambda+Z_t)r_t + \lambda z_t} = (2\pi)^{-3} \int \frac{8\pi(\lambda+Z_t)}{(p^2 - 2i\lambda p_z + 2\lambda Z_t + Z_t^2)^2} \times e^{-i\vec{p}\cdot\vec{r}_t} d^3p . \tag{16}$$

Introducing the Fourier transform (16) and the inverse transform of Eq. (7) into space integral (12), and writing $t = z_R/v$ and $\epsilon = \epsilon_p - \epsilon_t$, we obtain for the transition amplitude

$$A_{1s\text{-}nlm}(\vec{b}, v) = \frac{iZ_p}{\sqrt{\pi}\,\Gamma(-i\eta Z_t)} \frac{Z_t^{3/2}}{(2\pi)^{9/2} v} \int g_{nlm}^*(\vec{q}) \frac{8\pi(\lambda+Z_t)\lambda^{-i\eta Z_t'-1}}{(p^2 - 2i\lambda p_z + 2\lambda Z_t + Z_t^2)^2} \times \exp\{i\epsilon\eta z_R - i\vec{v}\cdot\vec{r} + i\tfrac{1}{2}(1-2\alpha)v z_R - i\vec{p}\cdot(\vec{r}+\alpha\vec{R}) + i\vec{q}\cdot[\vec{r} - (1-\alpha)\vec{R}]\} d^3r\, dz_R\, d^3q\, d^3p\, d\lambda . \tag{17}$$

The $\vec{r}$ integration can now be done yielding a factor $(2\pi)^3\delta(\vec{q}-\vec{v}-\vec{p})$. Rewriting $\vec{R}=(\vec{b}, z_R)$, $\vec{p}=(\vec{p}_b, p_z)$, and $\vec{v}=(0, v)$ in cylindrical coordinates allows us to single out the z_R integration which gives a factor $2\pi\delta(p_z-p_{0z})$ with $p_{0z}=-\frac{1}{2}v+\epsilon\eta$. With these steps, eight integrations have been performed in Eq. (17) so that we are left with a three-dimensional integral for the transition amplitude

$$A_{1s\to nlm}(\vec{b}, v)=i\frac{2^{5/2}Z_pZ_t^{3/2}}{v\Gamma(-i\eta Z_t')}\int g^*_{nlm}(\vec{p}+\vec{v})\Big|_{p_z=p_{0z}}\frac{(\lambda+Z_t)\lambda^{-i\eta Z_t'-1}e^{-i\vec{b}\cdot\vec{p}_b}}{(p_b^2+p_{0z}^2-2i\lambda p_{0z}+2\lambda Z_t+Z_t^2)^2}\,d^2p_b\,d\lambda\,. \tag{18}$$

This expression cannot be easily reduced further. However, the ultimate goal is not $A_{1s\to nlm}$ but the total cross section

$$\sigma_{1s\to n}=\int\sum_{lm}|A_{1s\to nlm}(\vec{b}, v)|^2d^2b \tag{19}$$

for electron capture into a given principal shell n. When taking $|A_{1s\to nlm}|^2$ the number of integrations doubles to $d^2p_b\,d^2p_b'\,d\lambda\,d\lambda'$. By inserting into Eq. (19), the $\vec{b}$ integration can immediately be performed yielding the factor $(2\pi)^2\delta(\vec{p}_b-\vec{p}_b{}')$. Thus, while in Eq. (18) only the longitudinal parts $q_\parallel=q_\parallel'=p_{0z}+v$ of $\vec{q}$ and $\vec{q}\,'$ are fixed we now see that also their transverse parts $\vec{q}_\perp=\vec{q}_\perp'=\vec{p}_b$ are the same in both g functions occurring in Eq. (19). The g functions can, therefore, be combined with the subshell summation to give the left-hand side of Eq. (8) with vanishing momentum spread, i.e., $\vec{q}=\vec{q}\,'=\vec{p}_{0z}+\vec{v}+\vec{p}_b$. This implies $x=0$ on the right-hand side of Eq. (8) and $\sin nx/(n\sin x)=1$. Remembering the general arguments of Sec. II B which suggested that *within a certain approximation* only the diagonal part of the density matrix (3) or (8) should contribute to the cross section (while the behavior in the remaining domain is irrelevant) we now find that within the eikonal approximation this statement holds *rigorously*. By eliminating $q_n=Z_p/n$ with the aid of $\epsilon=\frac{1}{2}(Z_t^2-Z_p^2/n^2)$ we can write the right-hand side of Eq. (8) more conveniently as

$$\frac{2Z_p^3}{\pi^2n^3[p_b^2+(\frac{1}{2}v+\epsilon\eta)^2+Z_p^2/n^2]^2}=\frac{2Z_p^3}{\pi^2n^3(p_b^2+p_{0z}^2+Z_t^2)^2}\,. \tag{20}$$

Since the λ, λ' integrations from Eq. (18) still factorize in Eq. (19) they can be carried out[17] individually yielding

$$\sigma_{1s\to n}=(2\pi)^2\int\left|i\frac{(Z_pZ_t)^{5/2}}{n^{3/2}}\frac{8(2Z_t-2ip_{0z})^{i\eta Z_t'}}{v\sinh(\pi\eta Z_t')\Gamma(-i\eta Z_t')}\left(\frac{\eta Z_t^{-1}Z_t'}{2Z_t-2ip_{0z}}\frac{1}{(p_b^2+p_{0z}^2+Z_t^2)^2}+\frac{i(1+i\eta Z_t')}{(p_b^2+p_{0z}^2+Z_t^2)^3}\right)\right|^2d^2p_b\,. \tag{21}$$

Owing to the azimuthal symmetry the remaining integrations reduce to a single integral via $d^2p_b\to\pi dp_b^2$ and can be easily performed. Reinserting $p_{0z}=-\frac{1}{2}v+\epsilon\eta$ we arrive at the final result

$$\sigma_{1s\to n}(Z_t, Z_p, v)=\alpha_n(Z_t, Z_p, v)\,\sigma_{1s\to n}^{\mathrm{OBK}}(Z_t, Z_p, v)\,, \tag{22a}$$

where the OBK cross section has the usual form[1,2,4]

$$\sigma_{1s\to n}^{\mathrm{OBK}}(Z_t, Z_p, v)=\frac{2^8\pi Z_p^5Z_t^5}{5n^3v^2[Z_t^2+(\frac{1}{2}v-\epsilon\eta)^2]^5}\,, \tag{22b}$$

and the scaling factor is

$$\alpha_n(Z_t, Z_p, v)=\frac{\pi\eta Z_t'}{\sinh(\pi\eta Z_t')}\exp\left[-2\eta Z_t'\tan^{-1}\left(\frac{\frac{1}{2}v-\epsilon\eta}{Z_t}\right)\right]\left[1-\frac{5}{8}\frac{Z_t'}{Z_t}+\frac{5}{48}\frac{Z_t'^2}{Z_t^2}+\left(\frac{1}{6}Z_t'^2+\frac{5}{4}\frac{Z_t'}{Z_t}\epsilon-\frac{5}{12}\frac{Z_t'^2}{Z_t^2}\epsilon\right)\eta^2+\frac{5}{12}\frac{Z_t'^2}{Z_t^2}\epsilon^2\eta^4\right], \tag{22c}$$

with $\eta=1/v$ and $\epsilon=-\frac{1}{2}(Z_p^2/n^2-Z_t^2)$. Result (22) is exact within the prior form of the eikonal approximation stated in Eqs. (12)–(14). For a hydrogen target, $Z_t=Z_t'=1$, we get our previous result,[10] for $Z_p=Z_t=Z_t'=n=1$ we recover the result of Dewangan,[15] and for $Z_t'=0$ the OBK approximation. Equation (22) is subject to several limitations: As is well known,[1,2] for $v\to\infty$, the second Born term becomes dominant and hence Eq. (22) does not apply. On the low-energy side, limitations caused by the atomic representation and by Eq. (11) are discussed in Sec. IV.

B. Cross section for capture into continuum states

The methods developed in the preceding sections can be easily applied to describe electron capture into projectile-centered continuum states.

In collisions of energetic highly stripped ions one finds, both experimentally[18] and theoretically,[18] a group of electrons ejected into a narrow forward cone. In the laboratory system, these electrons have a velocity $\vec{v}_e$ close to the projectile velocity $\vec{v}$ and correspondingly, in the projectile frame their momentum $|\vec{k}|$ (in a.u.) is small compared to v. The situation is hence analogous to capture into a high principal shell n.

In the eikonal approximation, the transition amplitude is again given by Eq. (12) with $\varphi_{nlm}(\vec{r}_p)$ in Eq. (14) replaced by the Coulomb continuum function $\varphi_{\vec{k}}(\vec{r}_p)$ (with a δ-function normalization on the momentum scale) for outgoing electrons and with $\epsilon_p = \frac{1}{2}k^2$. Rather than using a partial wave expansion it is convenient to introduce a compact representation[19] of the momentum wave function defined in analogy to Eq. (1),

$$\tilde{\varphi}_{\vec{k}}(\vec{q}) = -\frac{1}{2\pi^2} N\left(\frac{Z_p}{k}\right) \times \lim_{\epsilon\to 0} \frac{d}{d\epsilon}\left(\frac{[q^2-(k+i\epsilon)^2]^{-iZ_p/k}}{[(\vec{q}-\vec{k})^2+\epsilon^2]^{-iZ_p/k}}\right), \tag{23}$$

with

$$N(Z_p/k) = \exp(-\tfrac{1}{2}\pi Z_p/k)\Gamma(1+iZ_p/k). \tag{24}$$

Since we are interested in the total cross section for a given momentum $|\vec{k}|$ we need the momentum density matrix $\rho_{\vec{k}}(\vec{q},\vec{q}\,')$ integrated over all directions $\hat{k}$ of electron emission in the projectile system. Following the discussion of Sec. II A we anticipate that $q \gg k$ and only the domain $\vec{q}=\vec{q}\,'$ contributes to the cross section. The density matrix derived from Eq. (23) then takes a very simple form

$$\rho_k(\vec{q},\vec{q}) = \int \tilde{\varphi}^*_{\vec{k}}(\vec{q})\tilde{\varphi}_{\vec{k}}(\vec{q})\, d\hat{k} = \frac{4Z_p^2|N(Z_p/k)|^2}{\pi^3(q^2-k^2)^4}, \quad q \neq k. \tag{25}$$

A similar density matrix is obtained for the functions $g_{\vec{k}}(\vec{q})$ defined, in analogy to Eq. (7), as the Fourier transform of $\varphi_{\vec{k}}(\vec{r}_p)/r_p$. By inserting g_k into the Schrödinger equation one derives

$$\int g^*_{\vec{k}}(\vec{q})g_{\vec{k}}(\vec{q})\, d\hat{k} = \frac{|N(Z_p/k)|^2}{\pi^3(q^2-k^2)^2}, \quad q \neq k. \tag{26}$$

It is obvious that an "effective wave function" analogous to Eq. (10) may be readily defined by taking the square roots of the right-hand sides of Eqs. (25) and (26). By construction, the wave functions exhibit spherical symmetry and, of course, may be transformed back into coordinate space.

The calculation of the transition amplitude follows step by step the corresponding calculation in Sec. III A. When use is made of Eq. (26) with q^2 being fixed by the preceding reduction, a relation analogous to Eq. (20) shows that the denominator is indeed positive definite. Hence the integrand has no singularities in the whole range of integration.

As a result, we obtain the eikonal cross section for continuum electron capture into the momentum interval between k and $k+dk$ with respect to the projectile

$$\sigma_{1s\text{-}k}k^2 dk = \alpha_k(Z_t, Z_p, v)\sigma^{\mathrm{OBK}}_{1s\text{-}k}k^2\, dk, \tag{27a}$$

where α_k is given by Eq. (22c) with $\epsilon = \frac{1}{2}(k^2+Z_t^2)$ and the OBK cross section for continuum electron capture is

$$\sigma^{\mathrm{OBK}}_{1s\text{-}k} = \frac{2^{17}v^8 Z_p^2 Z_t^5 |N(Z_p/k)|^2}{5[v^4 - 2(k^2-Z_t^2)v^2 + (k^2+Z_t^2)]^5}, \tag{27b}$$

with

$$\left|N\left(\frac{Z_p}{k}\right)\right|^2 = \frac{\pi Z_p \exp(\pi Z_p/k)}{k\sinh(\pi Z_p/k)}. \tag{27c}$$

This expression is exact within the eikonal approximation, but again it should be kept in mind that the condition (11) has to be satisfied. Therefore, Eq. (27) is valid only for sufficiently small momenta k. In fact, unless $k \ll \frac{1}{2}v$ the very concept of projectile-centered wave functions does not apply and one then has to treat the full three-body problem. Our treatment is different from the standard OBK treatment[18] of continuum capture. (i) We allow for $k \neq 0$ and therefore have to perform an angular integration. For this reason, there is no direct simple relation between k and the velocity v_e in the laboratory system. (ii) The eikonal treatment leads to a scaling factor α_k (with respect ot the OBK cross section) which is similar in magnitude to the scaling factor for bound state charge capture.

IV. DISCUSSION OF THE RESULTS

A. Electron capture from hydrogen targets

Atomic hydrogen targets are the most important ones from the viewpoint of applications in plasma physics and for an understanding of the basic process. The capture cross section (22) for $Z_t = Z_t' = 1$ applies to a specific principal shell n. Experimentally, however, it is often not possible to specify the final electronic state, so that all bound states contribute to the cross section. Figure 1 shows the relative contributions of the various n shells to charge capture by fully stripped carbon ions. It is seen that for not too high projectile energies a great number of principal shells contribute with a maximum in the vicinity of the resonant transition $\epsilon = 0$ or $n = Z_p$. Only

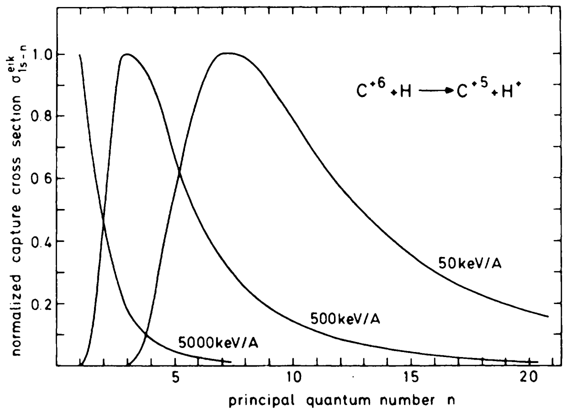

FIG. 1. Relative contributions of various principal shells n to the total cross section for electron capture from hydrogen into C^{6+} are plotted for three different projectile energies per nucleon. Between the integer values of n smooth curves have been drawn to guide the eye. The peak heights of the curves are normalized to 1.

for very high energies (when the cross section is already quite small) the higher momentum tails of the lower shells rather than the resonance condition dominate the cross section.

In order to account for the contributions from all principal shells it is useful to introduce a theoretical scaling factor $\alpha(Z_p, v)$ through the relation

$$\sigma_{capt} = \sum_n \sigma_{1s\text{-}n}(Z_p, v)$$

$$= \alpha(Z_p, v) \sum_n \sigma^{OBK}_{1s\text{-}n}(Z_p, v) . \quad (28)$$

The numerical calculations show that the theoretical scaling factor is almost independent of the projectile charge Z_p, see Table I. This is easily understood because in Eq. (22c), Z_p enters only through the energy difference ϵ, and ϵ is always

TABLE I. Calculated scaling factors $\alpha(1, Z_p, v)$ for hydrogen targets as a function of the projectile charge Z_p, and energy E per atomic mass unit. The first line shows the resonant scaling factor ($\epsilon = 0$) for comparison.

E (keV/amu)	50	100	200	500	1000	5000
$\epsilon = 0$	0.12	0.16	0.21	0.27	0.31	0.39
Z_p						
1	0.15	0.18	0.22	0.27	0.31	0.39
2	0.16	0.18	0.20	0.25	0.30	0.39
5	0.16	0.18	0.20	0.25	0.28	0.36
10	0.16	0.18	0.20	0.25	0.28	0.35
20	0.16	0.17	0.20	0.25	0.28	0.35

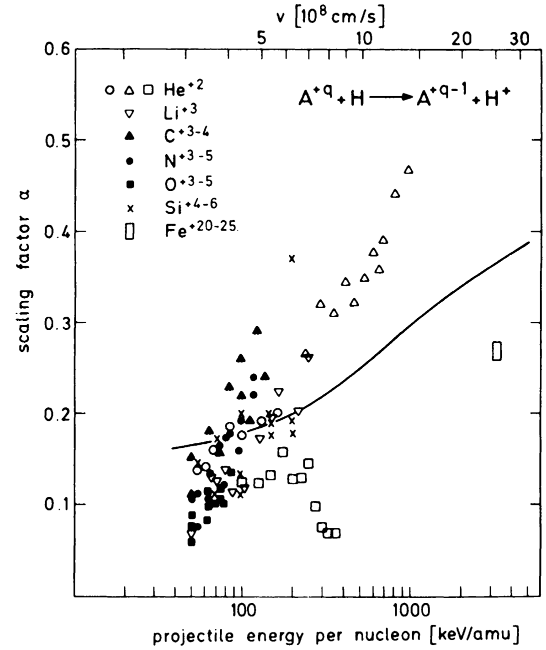

FIG. 2. Scaling factor obtained by dividing capture cross sections by the corresponding OBK cross section is plotted as a function of the projectile energy. The curve shows the theoretical result of Eq. (22c) for the representative charge $Z_p = 2$. The points indicate experimental data. Open circles, squares, triangles, and inverted triangles refer to Refs. 20, 21, 22, and 23, respectively. The data for partially stripped ions C, N, and O are from Ref. 24, for Si from Ref. 25. Points for different charge states of a given projectile are represented by the same symbol. The effective charges q_{eff} given by Olson and Salop (Refs. 8 and 25) have been used to calculate the OBK cross sections (C^{3+}: 2.4; C^{4+}: 3.2; N^{3+}: 2.5; N^{4+}: 3.2; N^{5+}: 4.1; O^{3+}: 2.6; O^{4+}: 3.4; O^{5+}: 4.3; Si^{4+}: 3.0; Si^{5+}: 4.1; Si^{6+}: 5.1). The data for Fe^{q+} with $q = 20$–25 are from Ref. 26. All six experimental points fall into the bar indicated if $Z_p = q$ is used to calculate σ^{OBK}. The data of Refs. 21, 22, and 26 refer to H_2 and have been divided by a factor of 2 for a reduction to atomic hydrogen.

associated with $\eta = 1/v$. Hence, at low-projectile energies when η is appreciable each projectile finds its appropriate resonance at $n \approx Z_p$, $\epsilon \approx 0$, while at high energies when ϵ is appreciable (cf. Fig. 1) η is small. In both cases, the ϵ independent terms in $\alpha_n(Z_p, v)$ dominate. In fact, taking $\epsilon = 0$ in Eq. (22c) gives a pretty good estimate for $\alpha(Z_p, v) \approx \alpha(v)$ defined by Eq. (28), see Table I.

In Fig. 2 we show[10] the energy dependence of the theoretical scaling factor for the representative projectile charge $Z_p = 2$. Also plotted are experimental data points[20-26] obtained by dividing the experimental capture cross section σ_{capt}(expt) by the summed OBK cross section $\sum_n \sigma^{OBK}_{1s\text{-}n}$. For partially stripped projectiles we have used effective charges (as given by Olson and Salop[8]) for calculating σ^{OBK}. The data are derived from a large number of measurements with various projectiles and various charge states. Before reduction, the corresponding cross sections range over many orders of magnitude. The experimental uncertainty is in most cases of the order of 30%. In view of the sensitivity of the plot the data all falls into a relatively narrow domain around our theoretical curve.

B. Capture of 1s electrons from multielectron targets

For multielectron targets, we adopt the following simple picture: The captured ("active") 1*s* electron moves in a Coulomb field produced by the effective target charges Z_t in the initial state (entering only through the binding energy) and Z_t' in the final state (entering only through the eikonal phase). All other electrons including the second ("passive") 1*s* electron do not change their orbits during the reaction. Although, for large separations, the active electron only sees the net charge 1 of the residual target ion it will be a good approximation, in most cases, to put $Z_t'=Z_t$ because small separations are weighted most heavily in the transition amplitude (12). We take this point of view but Eq. (22) offers more flexibility.

In order to be able to apply Eq. (22) two conditions have to be satisfied: (i) The atomic representation requires that the impact velocity v be greater than the orbital velocity v_K of the initially bound 1*s* electron (ii) The eikonal approximation requires that $\epsilon\eta/(\pi Z_t) \ll 1$ [cf. Eq. (11)]. Usually condition (i) is more restrictive. It suggests to introduce v/v_K or the projectile energy per nucleon divided by Z_t^2 as a parameter to characterize a collision system.

In Table II we present the calculated scaling factors for He, Ne, and Ar targets (taking bare charges $Z_t=Z_t'=2$, 10, and 18, respectively) and a variety of projectile charges Z_p. It is seen that the scaling factor is a function of v/v_K, which is

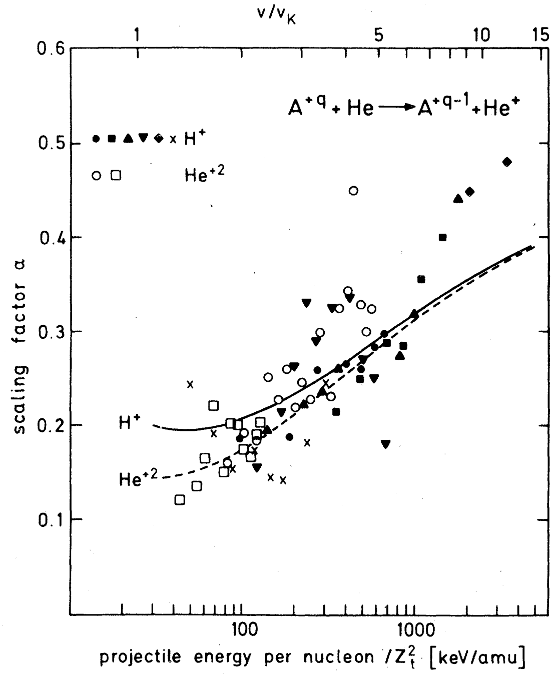

FIG. 3. For a helium target the scaling factor α obtained by dividing the total capture cross section by the corresponding OBK cross section is plotted as a function of the projectile energy per nucleon divided by Z_t^2 with $Z_t=Z_t'=1.6875$. The solid and the dashed lines show theoretical results for $Z_p=1$ and $Z_p=2$, respectively. The points indicate experimental data. Closed circles, squares, triangles, inverted triangles, diamonds, and crosses refer to Refs. 27, 28, 29, 30, 31, and 32, respectively. Open circles and squares refer to Refs. 22 and 21, respectively.

TABLE II. Calculated scaling factors $\alpha(Z_t, Z_p, v)$ for He, Ne, and Ar targets and various projectiles as a function of the projectile energy per nucleon divided by the square of the target charge number Z_t. The ratio v/v_K between the projectile velocity and the velocity of the target K electron is also given. In all cases bare target charge $Z_t=Z_t'$ have been used.

E/Z_t^2 (keV/amu)		50			100			200			500			1000	
v/v_K		1.41			2.00			2.83			4.47			6.32	
Target / Z_p	He	Ne	Ar	He	Ne	Ar	He	Ne	Ar	He	Ne	Ar	He	Ne	Ar
1	0.21	0.24	0.24	0.21	0.23	0.23	0.23	0.24	0.24	0.28	0.28	0.28	0.32	0.32	0.32
2	0.15	0.23	0.24	0.15	0.22	0.23	0.22	0.24	0.24	0.27	0.28	0.28	0.31	0.32	0.32
3	0.16	0.23	0.24	0.16	0.22	0.23	0.20	0.24	0.24	0.26	0.28	0.28	0.30	0.32	0.32
5	0.16	0.21	0.23	0.16	0.21	0.22	0.20	0.23	0.24	0.24	0.28	0.28	0.29	0.32	0.32
10	0.16	0.15	0.20	0.16	0.18	0.21	0.20	0.22	0.23	0.25	0.27	0.28	0.28	0.31	0.32
15	0.16	0.16	0.17	0.16	0.17	0.19	0.20	0.20	0.22	0.25	0.26	0.27	0.28	0.30	0.31
20	0.16	0.16	0.15	0.16	0.18	0.18	0.20	0.20	0.21	0.25	0.25	0.27	0.28	0.30	0.31

approximately independent of Z_p and Z_t. The reasons are the same as discussed in Sec. IV A.

Figure 3 shows the energy dependence of the theoretical scaling factor for the capture reactions $H^+ + He(1s^2) \rightarrow H + He^+(1s)$ and $He^{2+} + He(1s^2) \rightarrow He^+ + He^+(1s)$. For the screened target charges we have taken the standard[1] values $Z_t = Z_t' = 1.6875$. Also plotted are experimental data points obtained by dividing the experimental capture cross sections[21,22,27-32] by twice (for the two 1s electrons) the corresponding total OBK cross section. Similarly as in Fig. 2, the agreement is very satisfactory regarding the sensitivity of our plot and the simplicity of our theory.

For target atoms heavier than helium systematic measurements with high-energy projectiles (such that $v/v_K \gtrsim 1.5$ or $E/(Z_t^2 A) \gtrsim 50$ keV) are needed.

V. CONCLUDING REMARKS

In the present work, we develop an approach[10] to electron capture into arbitrary principal shells and into continuum states of the projectile. The approach is based on the momentum density matrix $\rho(\vec{q}, \vec{q}')$ of the captured electron summed over all substates, l, m or integrated over all emission angles, respectively. As a starting point, we rewrite the density matrix in a form which clearly exhibits its dependence on the "momentum spread" $|\vec{q} - \vec{q}'|$. We then proceed to give arguments that for electron capture it should be a good approximation to replace $\rho(\vec{q}, \vec{q}')$ by $\rho(\vec{q}, \vec{q})$ everywhere in momentum space because owing to the particular capture kinematics only the domain $\vec{q} \approx \vec{q}'$ contributes to the total cross section. This approximation[10] should be valid for any approach to electron capture. As an example, we treat the eikonal theory in its prior form. We discover that in this case the replacement prescription leads to an exact result. As a consequence, it is possible to calculate the eikonal cross section both for capture into arbitrary principal shells and into projectile-centered continuum states without further approximation. The final formula is a simple analytical expression factorizing into the well-known OBK cross section times a scaling factor $\alpha = 0.1 - 0.4$. This scaling factor turns out to be a function of v/v_K, approximately independent of the projectile and target charges. In view of its simplicity and better foundation our final formula should replace the OBK expression as a starting point for further refinements. Comparison with existing experimental data shows surprisingly good agreement. More precise data over a wider energy range and for a variety of targets and projectiles are needed to assess the limitations of our formula. In the meantime it may serve to estimate unknown cross sections needed for plasma research.

---

*Also Fachbereich Physik, Freie Universität Berlin.
†On leave from the Physics Dept., Univ. of Arkansas, Fayetteville, Ark. 72701.

[1] M. C. R. Mc Dowell and J. P. Coleman, *Introduction to the Theory of Ion-Atom Collisions* (North-Holland, Amsterdam, 1970).
[2] R. A. Mapleton, *Theory of Charge Exchange* (Wiley, New York, 1972).
[3] For a recent review, see D. Basu, S. C. Mukherjee, and D. P. Sural, Phys. Rep. 42C, 145 (1978).
[4] R. M. May, Phys. Rev. 136, A669 (1964).
[5] K. Omidvar, Phys. Rev. 153, 121 (1967); J. E. Golden, J. H. McGuire, and K. Omidvar, *ibid.* 18, 2373 (1978).
[6] V. Fock, Z. Phys. 98, 145 (1935).
[7] V. S. Nikolaev, Zh. Eksp. Teor. Fiz. 51, 1263 (1966) [Sov. Phys. JETP 24, 847 (1967)]; A. M. Halpern and J. Law, Phys. Rev. Lett. 31, 4 (1973). These references refer to scaling which for a given multielectron target is approximately independent of the projectile charge.
[8] R. E. Olson and A. Salop, Phys. Rev. A 16, 531 (1977).
[9] R. E. Olson, K. H. Berkner, W. G. Graham, R. V. Pyle, A. S. Schlachter, and J. W. Stearns, Phys. Rev. Lett. 41, 163 (1978).
[10] F. T. Chan and J. Eichler, Phys. Rev. Lett. 42, 58 (1979).
[11] K. Omidvar, Phys. Rev. A 12, 911 (1975).
[12] See, e.g., M. Kleber and M. A. Nagarajan, J. Phys. B 8, 643 (1975).
[13] R. J. Glauber, *Lectures in Theoretical Physics*, edited by W. E. Brittin *et al.* (Interscience, New York, 1959), Vol. I, p. 315; E. Gerjuoy and B. K. Thomas, Rep. Prog. Phys. 37, 1345 (1974).
[14] A. Tsuji and H. Narumi, J. Phys. Soc. Jpn. 41, 357 (1976).
[15] (a) D. P. Dewangan, J. Phys. B 8, L119 (1975); and 10, 1053 (1977). In this work, the post form of the eikonal approximation is used. Adopting the Gau-Macek phase [see (b) J. N. Gau and J. Macek, Phys. Rev. A 10, 522 (1974)] with an incorrect sign the author obtains a result for capture into the 1s state which he would have gotten from a correct treatment of the prior form of the eikonal approximation.
[16] R. N. Madan, Phys. Rev. A 11, 1968 (1975).
[17] I. S. Gradshteyn and I. M. Ryzhik, *Tables of Integrals, Series, and Products*, 4th ed. (Academic, New York, 1965), p. 285, Eq. 3.194 (6).
[18] G. B. Crooks and M. E. Rudd, Phys. Rev. Lett. 25,

1599 (1970); A. Salin, J. Phys. B 2, 631 (1969); 2, 1255 (1969); J. Macek, Phys. Rev. A 1, 235 (1970); K. Dettmann, K. G. Harrison, and W. M. Lucas, J. Phys. B 7, 269 (1974).
[19]H. A. Bethe and E. E. Salpeter, *Quantum-Mechanics of One- and Two-Electron Atoms* (Academic, New York, 1957); see Eq. (9.12).
[20]R. E. Olson, A. Salop, R. A. Phaneuf, and F. W. Meyer, Phys. Rev. A 16, 1867 (1977).
[21]L. I. Pivovar, M. T. Novikov, and V. M. Tubaev, Zh. Eksp. Teor. Fiz. 42, 1490 (1962) [Sov. Phys. JETP 15, 1035 (1962)].
[22]P. Hvelplund, J. Heinemeier, E. Horsdal Pedersen, and F. R. Simpson, J. Phys. B 9, 491 (1976).
[23]M. B. Shah, T. V. Goffe, and H. B. Gilbody, J. Phys. B 11, L233 (1978).
[24]R. A. Phaneuf, F. W. Meyer, and R. H. McKnight, Phys. Rev. A 17, 534 (1978).
[25]H. J. Kim, R. A. Phaneuf, F. W. Meyer, and P. H. Stelson, Phys. Rev. A 17, 854 (1978).
[26]K. H. Berkner, W. G. Graham, R. V. Pyle, A. S. Schlachter, and J. W. Stearns, Phys. Lett. 62A, 407 (1977).
[27]L. H. Toburen, M. Y. Nakai, and R. A. Langley, Phys. Rev. 171, 114 (1968).
[28]U. Schryber, Helv. Phys. Acta 40, 1023 (1968).
[29]L. M. Welsh, K. H. Berkner, S. N. Kaplan, and R. V. Pyle, Phys. Rev. 158, 85 (1967).
[30]J. F. Williams, Phys. Rev. 157, 97 (1967).
[31]K. H. Berkner, S. N. Kaplan, G. A. Paulikas, and R. V. Pyle, Phys. Rev. 140, A729 (1965).
[32]C. F. Barnett and H. K. Reynolds, Phys. Rev. 109, 355 (1958).